Nonlinear finite element analysis for structural capacity of railway prestressed concrete sleepers with rail seat abrasion

You, Ruilin; Goto, Keiichi; Ngamkhanong, Chayut; Kaewunruen, Sakdirat

DOI:
10.1016/j.engfailanal.2018.08.026

Document Version
Peer reviewed version

Citation for published version (Harvard):
You, R, Goto, K, Ngamkhanong, C & Kaewunruen, S 2019, 'Nonlinear finite element analysis for structural capacity of railway prestressed concrete sleepers with rail seat abrasion', *Engineering Failure Analysis*, vol. 95, pp. 47-65. https://doi.org/10.1016/j.engfailanal.2018.08.026

Nonlinear Finite Element Analysis of Structural Capacity of Railway Prestressed Concrete Sleepers with Rail Seat Abrasion

Ruilin You [a,b], Keiichi Goto [b,c] , Chayut Ngamkhanong [b], Sakdirat Kaewunruen [b*]
[a]Railway Engineering Institute, China Academy of Railway Sciences, Beijing 100081, China
[b]School of Engineering, the University of Birmingham, Birmingham B15 2TT UK
[c]Railway Technical Research Institute, Tokyo 2-8-38, Japan
*****Correspondence: s.kaewunruen@bham.ac.uk; Tel.: +44 (0) 1214 142 670

Abstract: Prestressed concrete sleepers are the most commonly used type of railway sleepers in ballasted railway track. They have a strong influence on track performance, track stiffness and railway safety. Reportedly in many railway lines (especially in heavy-rail networks), many prestressed concrete sleepers have failed due to rail seat abrasion (RSA). RSA is a wear deterioration of the concrete underneath the rail that results in various problems such as loss of fastening toe load, gauge variation, improper rail cant, and eventually loss of rail fastening. In addition, the RSA will directly decrease the capacity of worn concrete sleepers. However, to the best of authors' knowledge, there were very few studies that quantitatively examined the effects of RSA on the structural capacity of the prestressed concrete sleepers. In this paper, a numerical study is executed to evaluate the load-carrying capacity of a prestressed concrete sleeper using LS-DYNA. The nonlinear model was validated firstly based on theoretical analysis and experimental results in accordance with Australian Standard. Using the validated finite element model, the influences of different wear depth of RSA are investigated; and different compression strength and tensile strength of concrete and the prestress losses are highlighted. The outcomes of

this study lead to better insight into the influences of RSA more clearly and improve track maintenance and inspection criteria.

Keywords: Railway track; prestressed concrete sleeper; rail seat abrasion; load capacity; numerical analysis; finite element method; LS-DYNA

1. Introduction

Prestressed concrete sleepers are one of the most important components in ballasted railway tracks [1-3]. Prestressed concrete sleepers lie between the rail and ballast, to transfer the train's loads from the wheel to the rail, and the rail to the ballast bed; and then to secure rail gauge and keep the geometry of railway line within a suitable range [4, 5]. Fig. 1 shows the prestressed concrete sleepers in ballasted railway track.

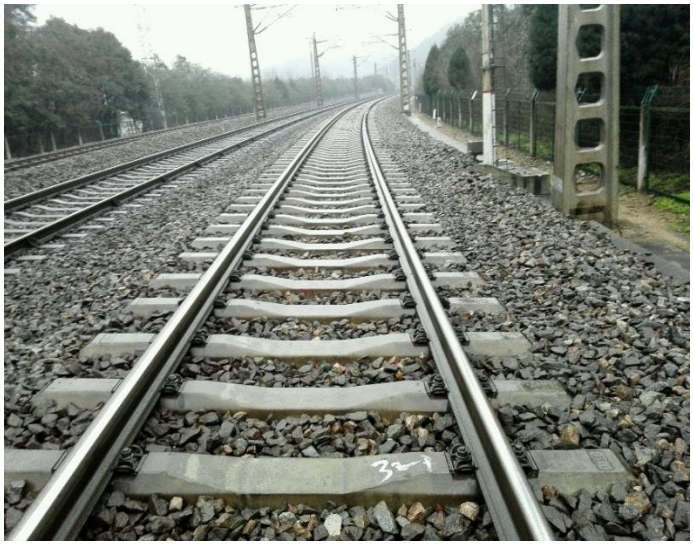

Fig. 1. Prestressed concrete sleepers in ballasted railway track

Prestressed concrete sleepers play a major role in track performance, track stiffness and operational safety. The performance deterioration of concrete sleepers is a safety-concerned question of operation and maintenance departments within the railway organisations. A sleeper failure in critical locations such as switches and

crossings, transom bridges, bridge ends, rail joints, and so on can lead to significant incidents in railway operations (e.g. train derailments, operational downtime, broken signaling equipment, etc.). Because it is rather different to predict the particular location of long continuous track where the sleeper will fail, the performance of concrete sleepers is generally defined by structural reliability obtained from the stress generated from repeat loads (or action) and sleepers' resistance (or capacity) [4]. In addition, the performance deterioration of concrete sleepers can be influenced by the lateral and vertical dynamic loads transferred from the rails, the manufacturing quality and maintenance defects, and the exposure to environmental conditions, etc. The most common problems related to concrete sleepers in North America and worldwide are surveyed and ranked in Table 1 [6, 7].

Table 1. Common damages of prestressed concrete sleepers (Ranked from 1 to 8, with 8 being the most critical) [6, 7]

Main Causes	Damages	North American rank	International rank
Lateral load	Abrasion of concrete material on rail seat	**6.43**	3.15
	Shoulder/fastening system wear or fatigue	6.38	5.5
Vertical dynamic load	Cracking from dynamic loads	4.83	5.21
	Derailment damage	4.57	4.57
	Cracking from centre binding	4.5	5.36
Manufacturing and maintenance defects	Tamping damage (or impact forces)	4.14	**6.14**
	Other (e.g. manufactured defect)	3.57	4.09
Environmental considerations	Cracking from environmental or chemical degradation	3.5	4.67

From Table 1, we can see that abrasion and cracking are the main damages of prestressed concrete sleepers [8]. Rail seat abrasion (RSA) is the wear degradation underneath the rail on the surface of prestressed concrete sleepers (Fig. 2).

Fig. 2. Typical RSA of prestressed concrete sleeper

RSA of a prestressed concrete sleeper can be related to the climatic and traffic conditions and the location of the concrete sleepers in the track. In particular, axle load, traffic volume, curvature and grade of the rail line, the presence of abrasive fines (e.g. locomotive sand or metal shavings), the behaviour of the fastening system, and climate are the key factors that contribute to RSA [9, 10]. Based on North American heavy railway network experiences and concrete sleeper tests results, heavy axle loads, abrasive fines, moisture, and rail movement appear to be the most important factors [11, 12].

In 2009, Zeman and Bakke did some research work on the mechanisms of RSA, based on their results, abrasion, crushing, freeze-thaw cracking, hydraulic pressure cracking, hydro-abrasive erosion and cavitation erosion were the potential mechanisms [11-14]. In 2010, a laboratory test apparatus and procedure were devised by Zeman to investigate the influence of hydraulic pressure cracking, hydro-abrasive erosion, and cavitation erosion, and several suggestions to mitigating RSA were given [9, 10]. Borg et al. performed large-scale abrasion tests in 2014 [15], based on the results of the experiments, they concluded that the frictional characteristics between a

rail pad and rail seat had an impact on the transfer of forces and relative movement and could influence RSA. Kaewunruen et al. [16] presented a nonlinear finite element model to evaluate influences of surface abrasions on dynamic behaviours of railway concrete sleepers.

RSA results in many problems of railway tracks such as loss of fastening toe load, gauge variation, improper rail cant, and eventually loss of rail fastening. There are many researches about RSA, from the literal review above, most of previous works focused on the mechanisms of RSA, however, there were very few studies that quantitatively examined the effects of RSA on the loading capacity of the prestressed concrete sleepers. This implies that the maintenance of sleepers cannot be properly scheduled or planned in advance. If fact, the sleepers are generally embedded in ballast, it is almost impossible to inspect structural damage such as cracks, which are the warning sign towards structural failure. One sleeper failure can definitely lead to another failure. Therefore, it is necessary to develop the engineering guideline to determine the structural integrity and capacity of the aging and worn railway sleepers with RSA. Without the insight into the structural capacity, the structural reliability of sleepers cannot be determined and their safety margin cannot be quantified. This implies that railway operations would be based purely on radical assumptions and crude estimates. This study is the world first to address this key challenge towards truly realistic condition-based predictive track maintenance. In this paper, a numerical study is rigorously executed to comprehensively evaluate structural capacity of railway prestressed concrete sleepers exposed to RSA.

2. Structural details of prestressed concrete sleeper

In this study, concrete sleepers subjected to bending moments according to AS 1085.14 [17] are analysed. The geometry details of the sleeper are shown in Fig. 3 [18-20]. The concrete sleeper meets all the technical requirements of AS 1085.14 [17], and the dimension of this sleeper is 2134 mm × 254 mm (bottom) × 183mm (rail seat), there are 18 prestressing steels (ϕ5.03 mm) in the sleeper. Stirrups (ϕ3 mm) are placed along the beam with a spacing of 200mm and a yield capacity of 350Mpa. There are two equal pressure loads at rail seat of the concrete sleeper during the test. Later, the prestressed concrete sleeper will be modelled, and the mechanical characteristics during the loading processes will be evaluated as well.

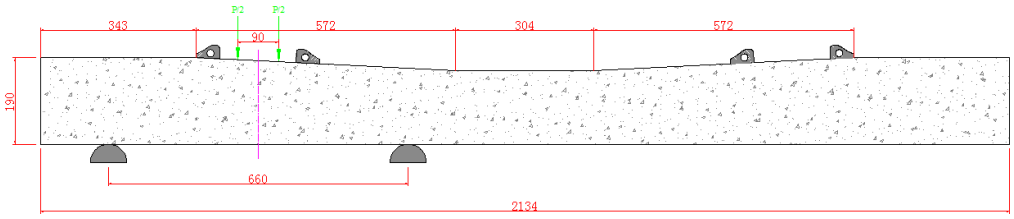

(a) Front view of the sleeper

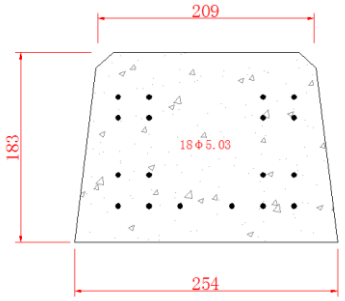

(b) Rail seat section

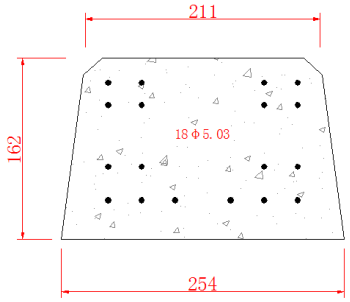

(c) Midspan section

Fig. 3. Concrete sleeper geometry details (Unit: mm)

For this prestressed concrete sleeper, the concrete's characteristic compressive strength is C70, and the 20% proof-stress yield strength of the prestressing steel is 1620MPa. The initial prestress-force in each steel tendon is 26.4kN, the prestress loss

rate is taken as 12% firstly, that means the efficient prestress-force in each steel tendon is 23.2kN, and the efficient prestress in each steel tendon is 1160Mpa accordingly. Similar to other prestressed concrete (PC) members, the prestress of concrete sleepers will be lost after being transferred, and the prestress loss will sustain during the life of sleeper, the prestress loss rate influence will be discussed later. Note that the materials' details are shown in Table 2.

Table 2. Materials properties [18, 19]

Material	Basic variables	symbol	Value
Concrete properties	Concrete mean compressive strength	f_{cm}	85MPa
	Concrete flexural tensile strength	f_{cf}	5.8MPa
	Concrete modulus of elasticity	E_c	43.8GPa
Prestressed wire properties	Ultimate tensile strength of prestressed steel	f_{pb}	1860MPa
	Yield strength of prestressed wire	f_{py}	1620MPa
	Modulus of elasticity of prestressed wire	E_s	200GPa

3. Finite element modelling strategies

3.1 Material models

The finite element models in this paper are established using the software package LS-DYNA developed by the Livermore Software Technology Corporation (LSTC) in 1976, which has been continuously developed ever since [21]. LS-DYNA® provides several 'simple input' concrete models for concrete using basic strength test data and thus reducing the burden of performing comprehensive tests on concrete to determine the complicate parameters [22]. The common used 'simple input' concrete models include *MAT_WINFRITH_CONCRETE, *MAT_CONCRETE_DAMAGE_REL3, *MAT_PSEUDO_TENSOR and *MAT_CSCM_CONCRETE [22]

In this study, the Winfrith Concrete Model is chosen to stimulate the concrete of the sleeper. The Winfrith Concrete Model is implemented in the 8-node single integration point continuum element, which was developed in the 1980s [23]. The most important capability of this model is the crack prediction details of concrete [24]. The model is based on the four-parameter model which was developed by Ottosen [25]. The Winfrith Concrete Model adopts the following functions:

$$Y(I_1,J_2,J_3) = aJ_2 + \lambda\sqrt{J_2} + bI_1 - 1 \qquad \text{(Eq.1)}$$

When $\cos 3\theta \geq 0$

$$\lambda = k_1 \cos\left[\frac{1}{3}\cos^{-1}(k_2 \cos(3\theta))\right] \qquad \text{(Eq.2)}$$

When $\cos 3\theta \leq 0$

$$\lambda = k_1 \cos\left[\frac{\pi}{3} - \frac{1}{3}\cos^{-1}(-k_2 \cos(3\theta))\right] \qquad \text{(Eq.3)}$$

Where

$$\cos(3\theta) = \frac{3\sqrt{3}}{2}\frac{J_3}{{J_2}^{3/2}} \qquad \text{(Eq.4)}$$

I_1 is the first invariant of stress tensor, which represents volumetric responses, J_2 and J_3 are the second and third invariants of deviatoric stress tensor and they account for deviatoric responses. a, b, k_1, and k_2 are functions of the ratio of tensile strength to compression strength and are determined from a variety of tests, including: uniaxial compression, uniaxial tension, biaxial compression, and triaxial compression.

In the model, *MAT_ELASTIC_PLASTIC_THERMAL is used to simulate the characteristics of prestressing steels. This is Material Type 4 [26]. Young's moduli and plastic hardening moduli can be defined at a different temperature to give the bilinear isotropic of prestressing steel. In addition, this material type can define nodal

temperatures by activating a coupled analysis or by using another option to define the temperatures such as *LOAD_THERMAL_LOAD_CURVE, or *LOAD_THERMAL_VARIABLE which is suitable to simulate the initial prestress in the prestressing steel [26].

The stirrups are modelled by Material Type 3, which is called *MAT_PLASTIC_KINEMATIC. This material model is computationally efficient and is suitable to model isotropic and hardening plasticity for the beam, shell and solid elements [26].

3.2 Finite element modelling

In this study, concrete and supports are modelled as solid elements, and all concrete elements meshed as a hexahedral solid element. Prestressed steels and the stirrups are modelled as a beam element. The support condition was modelled as pin-pin support in accordance with AS 1085.14 [17]. Fig. 4 shows the whole view of the finite model, Fig. 5 shows the prestressed steels and the stirrups in concrete.

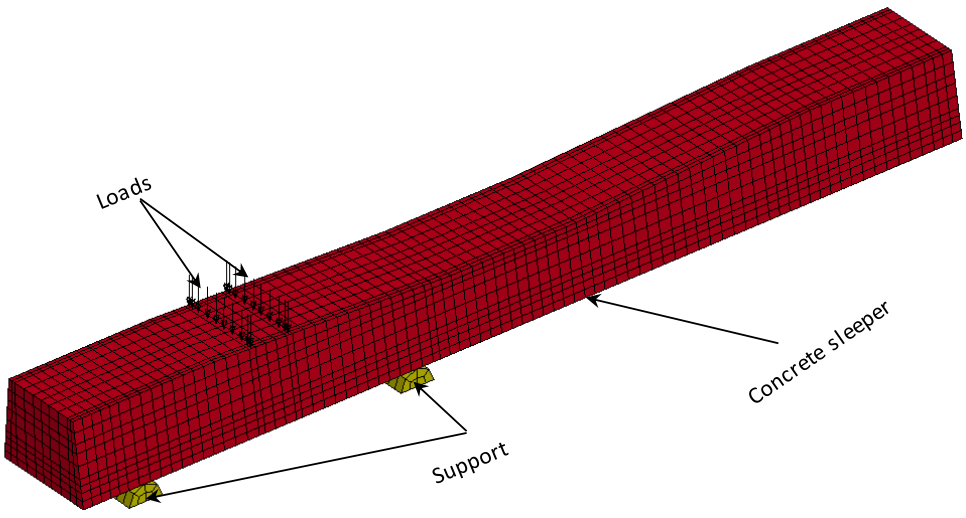

Fig. 4. The finite element model of concrete sleeper

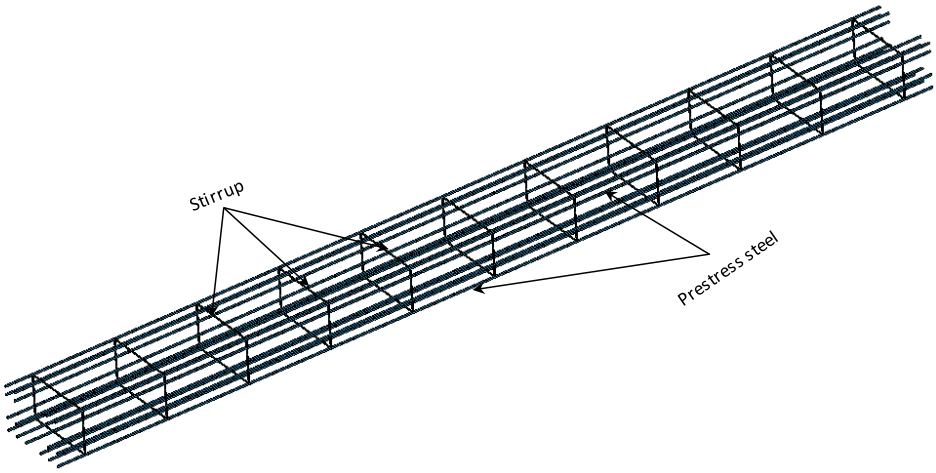

Fig. 5. The finite element model of prestressed steels and the stirrups in concrete

In the model, concrete, prestressed steels and stirrups are considered to be well adhered, and the Shared Nodes method is used to simulate the constraints between reinforcement and concrete. This is due to the fact that with relatively small prestressing tendons, the bond slip and bursting does not generally incur [4]. The shared node approach for including reinforcement requires the nodes of the reinforcement grid and concrete mesh to be identical.

Contact is considered between sleeper and support, and the keyword *CONTACT_AUTOMATIC_SURFACE_TO_SURFACE is used to deal with the contact relationship between concrete's elements and supports' elements. In this study, the rotations and translations of the supports are constrained as simple supports in the *MAT_RIGID (the material used for supports) parameters cards [26, 27]. The loading condition is to apply a uniform load directly on the concrete sleeper [28-30].

4.Finite element modelling validation

4.1 Loading process

Loading processes of prestressed concrete sleeper could be divided into two stages: prestressing force transfer (i.e. when releasing initial prestress during manufacturing) and test loading (i.e. when a sleeper experience external loads from train). In the stage of prestressing force transfer, the Keyword of *LOAD_THERMAL_VARIABLE is used to define the temperature in the model. It is reported that this thermal load case can be used to the prestress force transfer [21, 22]. In order to simulate the prestress force transforming process, the temperature is liner changed along the prestressing transforming length. The total time of prestressing force transforming process is 10ms. Fig. 6 shows the x-stress (longitudinal) distribution within the sleeper due to initial prestressing force.

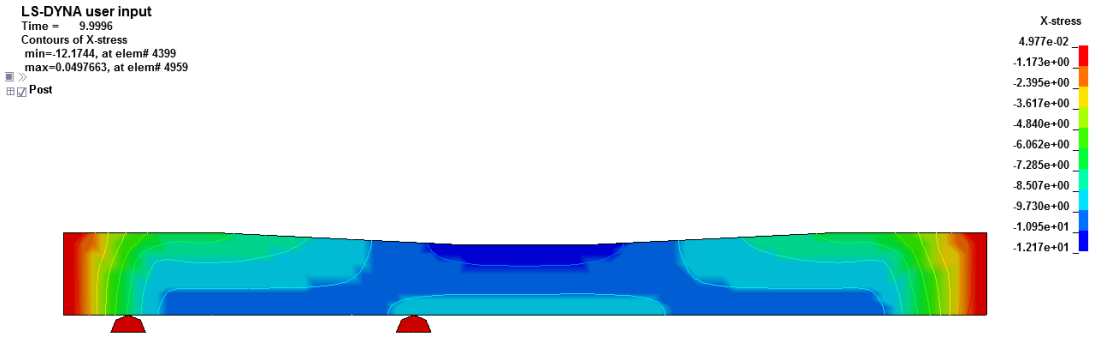

Fig. 6. X-stress of sleeper after transforming prestress force

After the prestress force transferred, the test load is applied to the sleeper using the Keyword *LOAD_SEGMENT_SET. The tensile stress of concrete at the bottom side of a sleeper at the rail seat is increasing with the testing load development until cracking. Then the concrete sleeper is loaded continually until reaching the ultimate

strength. In Fig. 7, the stress distribution in the concrete sleeper is visualized just after the first crack appears. Fig. 8 shows the deformation and the stress distribution of the sleeper just before failure.

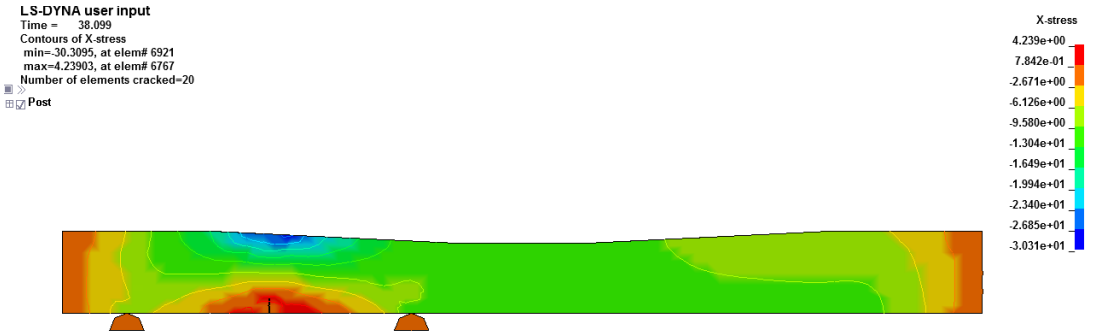

Fig. 7. X-stress of sleeper just after the first crack appears

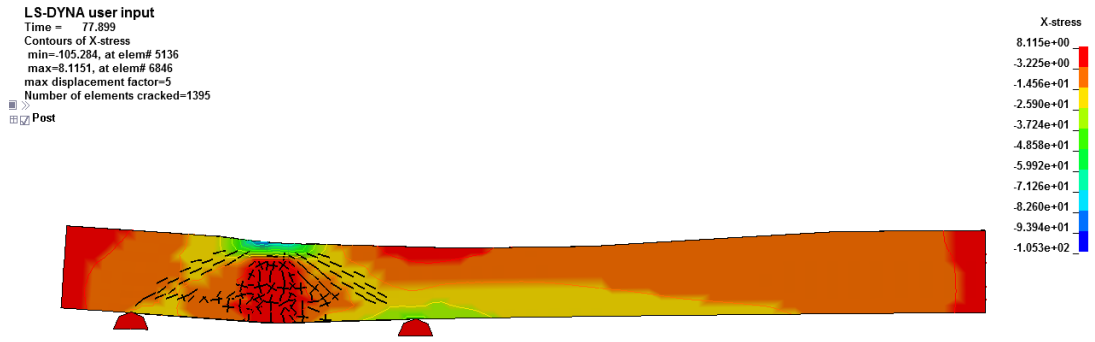

Fig. 8. Deformation and the stress distribution of the sleeper just before failure

4.2 Different mesh size model validation

In order to validate the finite element model, different mesh sizes were used in the model to analyze the mesh sensitivity of the model. The different nominal mesh sizes adopted for the mesh sensitivity study correspond to 20 mm, 30 mm, 40 mm. The load-deflection responses for the prestressed concrete sleeper at rail seat, based on different mesh size, are plotted in Fig. 9. From Fig. 9, it can be found that the load-deflection responses of different size-meshed models are similar and close to the

experiment results. It is clear that the finite element results have converged (when the mesh size is of 40mm or smaller), similar to previous analyses [4].

More details of the load-deflection responses of the 30mm size model are shown in Fig. 10. Not only does Fig. 10 reveal the processes of cracking and ultimate failure of a concrete sleeper but it also gives the processes of prestressing stress transferring and decompression of sleeper at the bottom side of rail seat. It is clear from the finite element analysis results that the response of the model is linear until the first crack has formed. After this point, the cracking sleeper deforms along with the increasing of the test load. The numerical model also can capture well the nonlinear load-deflection response of the concrete sleeper up to failure.

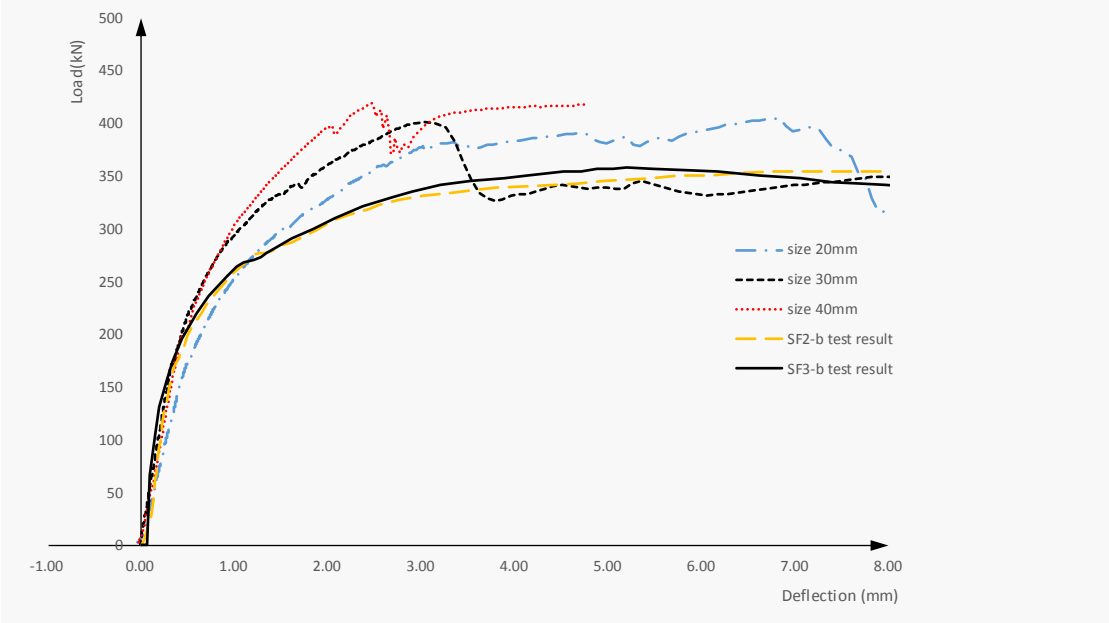

Fig. 9. Load-deflection responses of concrete sleeper at rail seat section

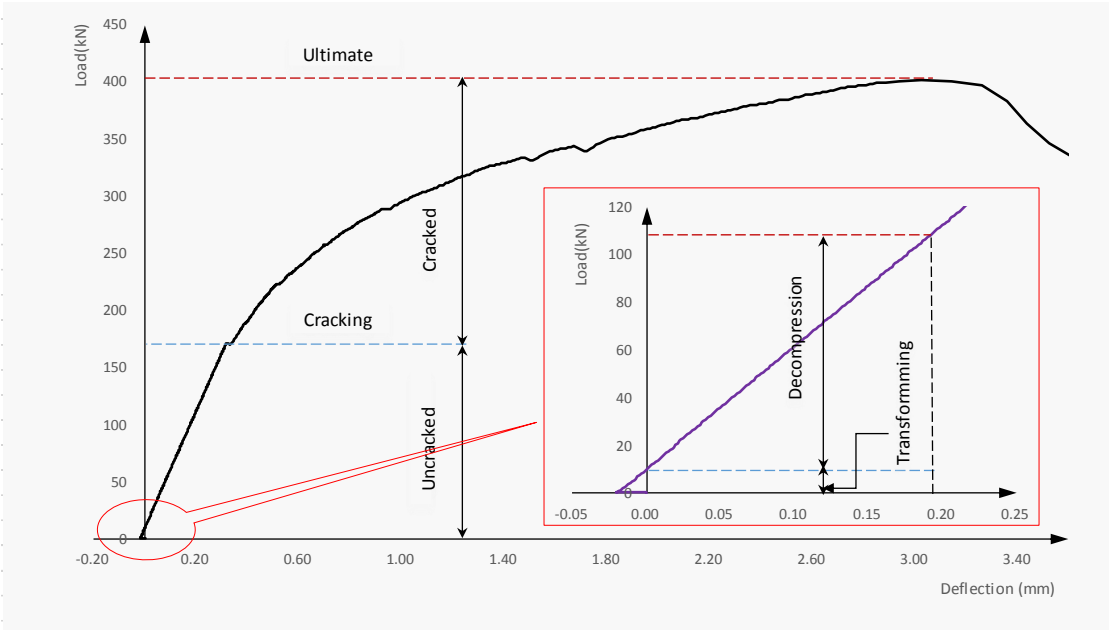

Fig. 10. Load-deflection responses of concrete sleeper at rail seat section (size 30mm)

In addition to the load-deflection characteristics, the FE-model could provide other behaviours of the concrete sleeper easily; this is one of the advantages of the simulation, compare to actual experiments. In this study, the stress changing process of the prestress steel on the bottom of rail seat section is shown in Fig. 11. Based on Fig.11, it can be found that the stress of the prestressing steel at the yield point is 1624MPa, at the fracture point is 1857MPa, and these results are in very good agreement with other simulation and experimental data.

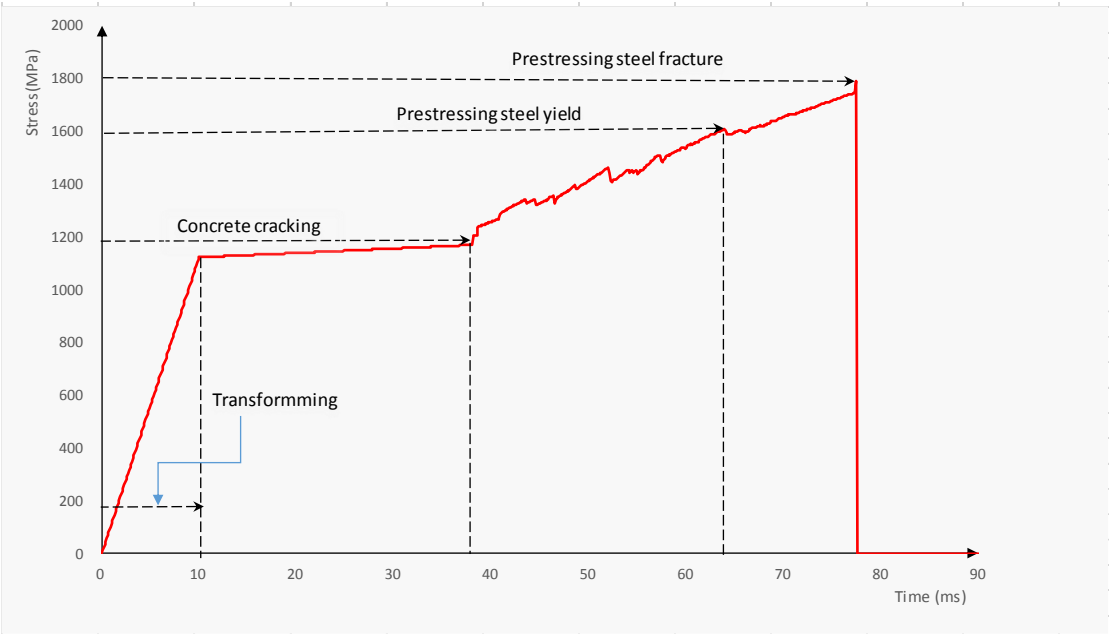

Fig. 11. Stress development in the prestress steel (size 30mm)

Based on the geometry of the concrete sleeper, the important cross sectional properties of the rail seat section are calculated and shown in Table 3. Using these parameters, the structural capacity of rail seat section can be calculated by theoretical analysis or standards recommended by a code of practice.

Table 3. Cross sectional properties of rail seat section

Parameters	**Gross concrete**	**Transformed section**
Modulus of elasticity ratio of prestressing wire and concrete n_e	5.33	
Eccentricity of the centroid of prestressing force e(mm)	-4.1	
Area (mm^2)$\times 10^3$	42.4	43.9
Distance from the centre of gravity of the section to the soffit y_b(mm)	89	88
First moment about the bottom fibre S_b(mm^3) $\times 10^3$	1247.6	1276.5
Moment of inertia of transformed section about its centroidal axis I_t(mm^4) $\times 10^6$	117.9	120.8

In order to verify the FE-model, the comparison between the numerical simulations, theoretical analyses and the experimental data are displayed in Table 4 and Table 5.

Table 4. Comparison cracking loads between the FE-model, theoretical analysis and experiment*

Specimen ID	Experiment [18, 19] (kN)	Theoretical analysis (kN)	Size 20mm		Size 30mm		Size 40mm	
			FE (kN)	Deviation	FE (kN)	Deviation	FE (kN)	Deviation
SF2-a	179	170	171	4%	173	3%	197	-10%
SF2-b	180			5%		4%		-9%
SF3-a	170			-1%		-2%		-16%
SF3-b	172			1%		-1%		-15%

* Deviation in the Table is the values that relative to experiment

Table 5. Comparison ultimate loads between the FE-model, theoretical analysis and experiment*

Specimen ID	Experiment [18, 19] (kN)	Theoretical analysis	Size 20mm		Size 30mm		Size 40mm	
			FE (kN)	Deviation to Experiment	FE (kN)	Deviation to Experiment	FE (kN)	Deviation to Experiment
SF2-b	355	358	40	-13%	40	-13%	41	-17%
SF3-b	357		2	-13%	1	-12%	7	-17%

* Deviation in the Table is the values that relative to experiment

Table 4 and Table 5 show that the simulation results could be well matched with the theoretical analyses (i.e. cross sectional analysis method) and experiment results. The comparison also shows that, compare to 40mm mesh-sized model, 20mm and 30mm mesh-sized models' results are closer to the experimental test results. Since the 30mm sized model's results are very close to 20mm sized model's, the elements' mesh size of 30mm has been chosen taking into account the time economy of calculation.

5. Influences of RSA

5.1 Dimension of the RSA

In order to study the influence of the rail seat abrasion, the concrete abrasion of concrete sleeper was simulated in the finite element model. The location and dimension of abrasion are shown in Fig. 12, the width of at the bottom of the abrasion

is 150mm (b), the same as the width of rail base. The depth (d) of abrasion is chosen as 10mm, 20mm and 30mm, to analyze the influence of different abrasion degrees.

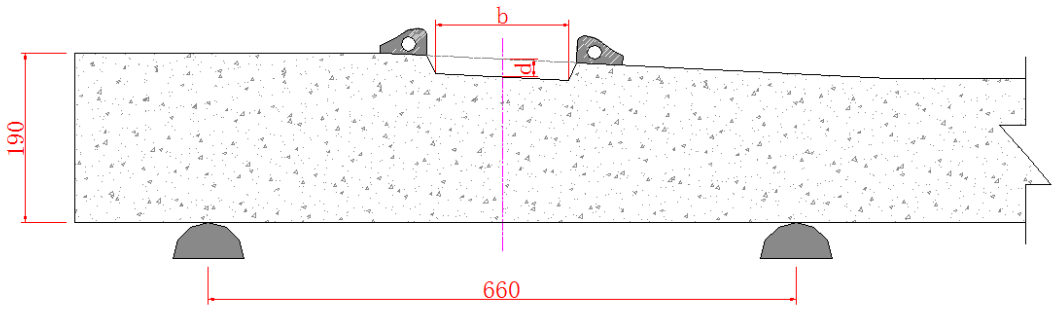

Fig. 12. The abrasion dimension is chosen in the finite element model

5.2 Simulation results and discussion

The load-deflection responses for the prestressed concrete sleeper at rail seat with various cases of different abrasion depths are shown in Fig. 13. Based on Fig. 13, it can be found that the increment of the abrasion depth reduces the stiffness of sleeper. It can be observed clearly that the deflection of the sleeper increased subject to the same load.

The cracking loads and ultimate loads are influenced by the depth of abrasion as well. The variable quantity of load capacity is given in Table 6. From Table 6, it could be found that the 10mm abrasion depth would decrease about 20kN cracking load for the rail seat section. The ultimate load of prestressed concrete sleepers is not decreased linearly according to the abrasion depth.

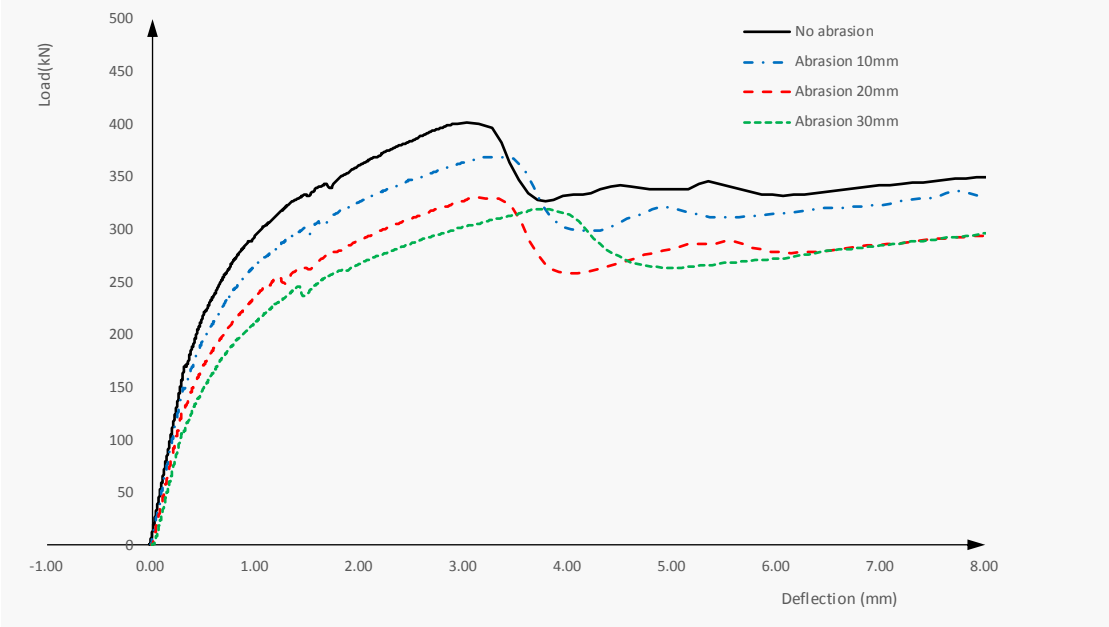

Fig. 13. Load-deflection responses of concrete sleeper due to different depth of RSA

Table 6. Loading capacity of prestressed concrete sleeper

Load type	No abrasion	Abrasion 10mm	Abrasion 20mm	Abrasion 30mm
Cracking load (kN)	173	149	126	106
Ultimate load(kN)	401	367	330	320

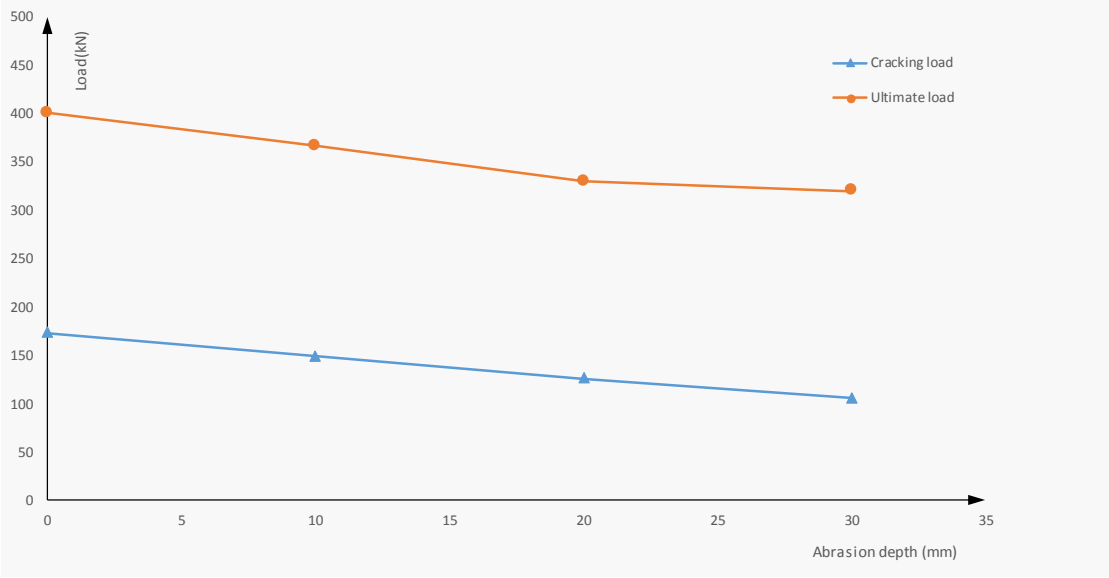

Fig. 13. Loading capacity of sleeper influenced by RSA

5.3 Parametric studies

Besides RSA, the structural capacity of a prestressed concrete sleeper is also influenced by material parameters and efficient prestress stress in concrete. In the

following section, based the validated finite element model, different compression strength and tensile strength of concrete and the prestress stress loss rate will be studied. In order to analyze each parameter's influence on the structural capacity of the sleeper alone, only one parameter will be changed at one time.

(1) Compression strength of concrete

Considering the compression strength of concrete from 40MPa to 85 MPa, the loading capacity of a sleeper is given in Table 7. The cracking loads and ultimate loads for the sleepers with different RSA depth are shown in Fig. 14 and Fig. 15 individually.

From Table 7, Fig. 14 and Fig. 15, it can be found that, with the development of the compression strength of concrete, the cracking load of a sleeper does not change whilst the ultimate load of the sleeper has slightly increased. This is because the cracking load of a sleeper is mostly depending on the tensile strength of concrete, the efficient prestress stress in concrete, and stress redistribution across the cross section. However, the ultimate load of a sleeper is largely influenced by the geometry of the cross section (e.g. cross sectional area), the ultimate tensile strength of prestressing steel tendons and the compression strength of concrete.

Table 7. Loading capacity of sleeper based on different compression strength of concrete

Compression strength(MPa)	**Cracking load for different RSA depth (kN)**				**Ultimate for different RSA depth (kN)**			
	0	**10mm**	**20mm**	**30mm**	**0**	**10mm**	**20mm**	**30mm**
40	170	148	125	105	387	335	312	298
50	170	149	126	105	390	346	316	302
60	170	149	126	105	392	358	318	308
70	171	149	126	106	404	361	324	310
80	171	149	126	106	399	364	326	311
85	173	149	126	106	401	367	330	320

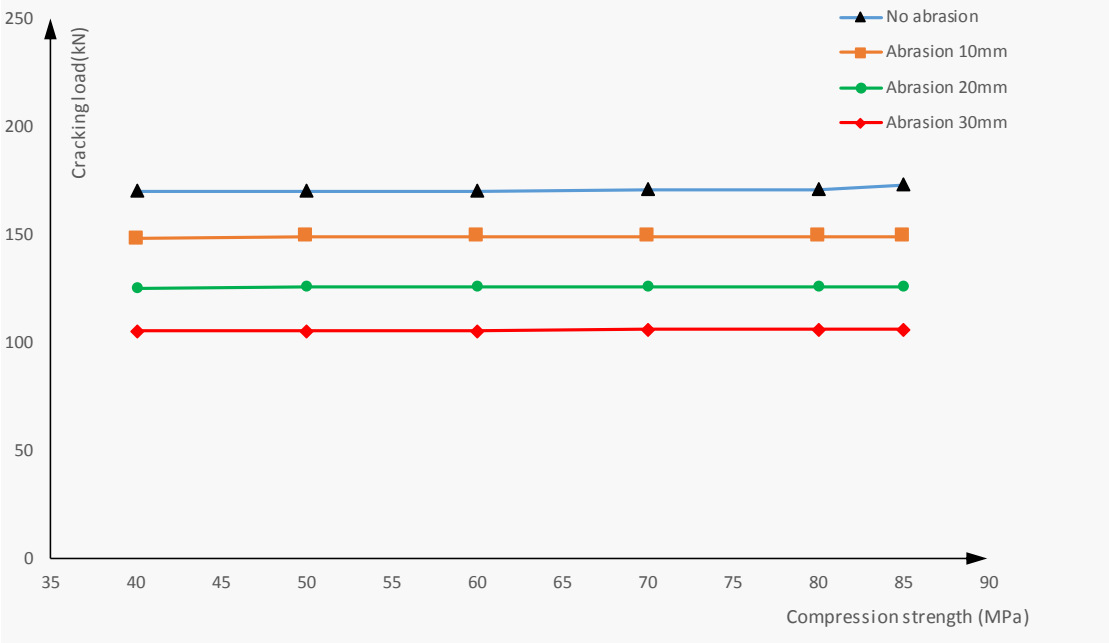

Fig. 14. Cracking load of sleeper influenced by compression strength of concrete

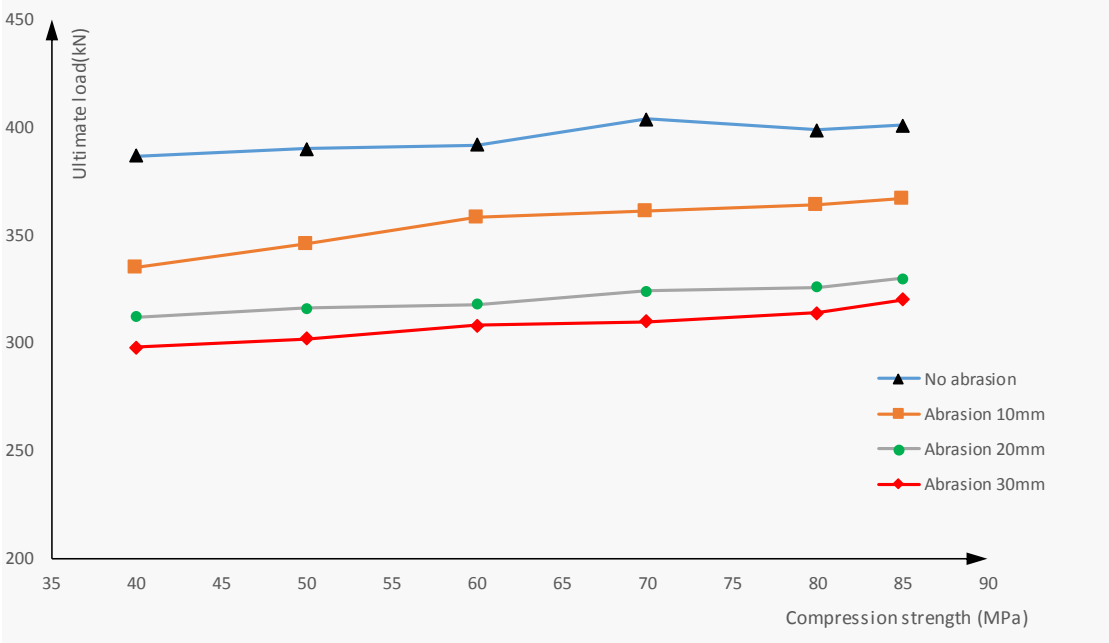

Fig. 15. Ultimate load of sleeper influenced by compression strength of concrete

(2) Tensile strength of concrete

By increasing the tensile strength of concrete from 2MPa to 5.7MPa, the loading capacity of sleepers with different depth RSA are given in Table 8. The cracking

loads and ultimate loads for the sleepers with different RSA depth are shown in Fig. 16 and Fig. 17.

Based on Table 8, Fig. 16 and Fig. 17, it can be found that, with the development of the tensile strength of concrete, the cracking load of a sleeper increases whilst the ultimate load of sleeper almost does not change. These results validate the cracking load of a sleeper is related directly to the tensile strength of concrete.

Table 8. Loading capacity of sleeper based on different tensile strength of concrete

Tensile strength (MPa)	**Cracking load for different RSA depth (kN)**				**Ultimate for different RSA depth (kN)**			
	0	**10mm**	**20mm**	**30mm**	**0**	**10mm**	**20mm**	**30mm**
2	134	115	96	81	404	375	336	303
3	143	127	104	88.2	414	386	339	309
4	154	134	113	95.6	413	377	340	311
5	164	143	120	101	405	367	337	316
5.7	173	149	126	106	401	370	338	320

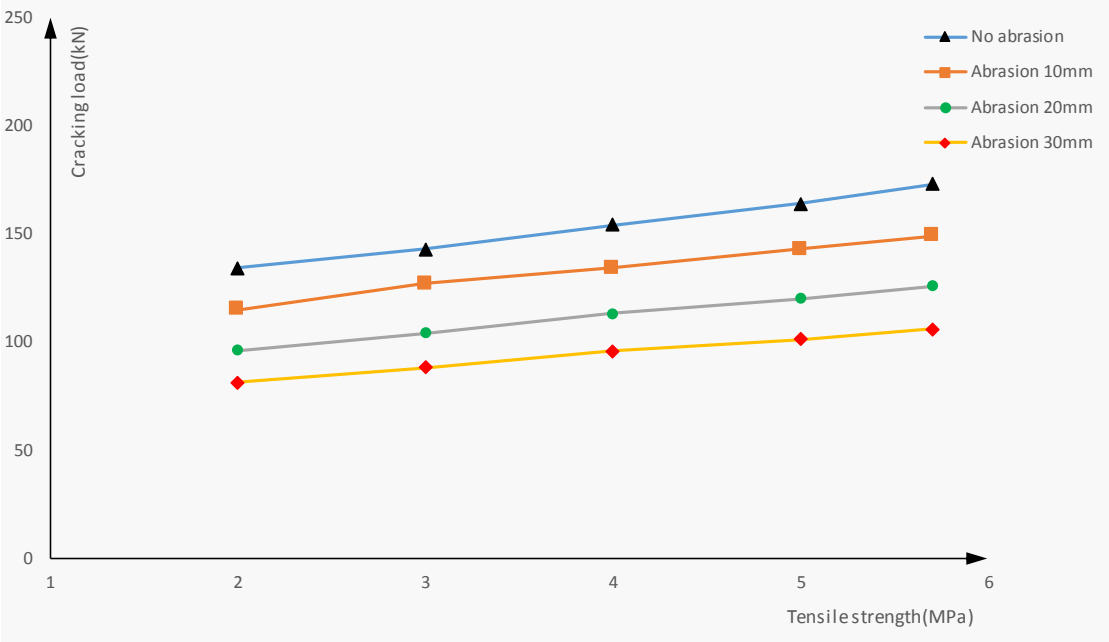

Fig. 16. Cracking load of sleeper influenced by tensile strength of concrete

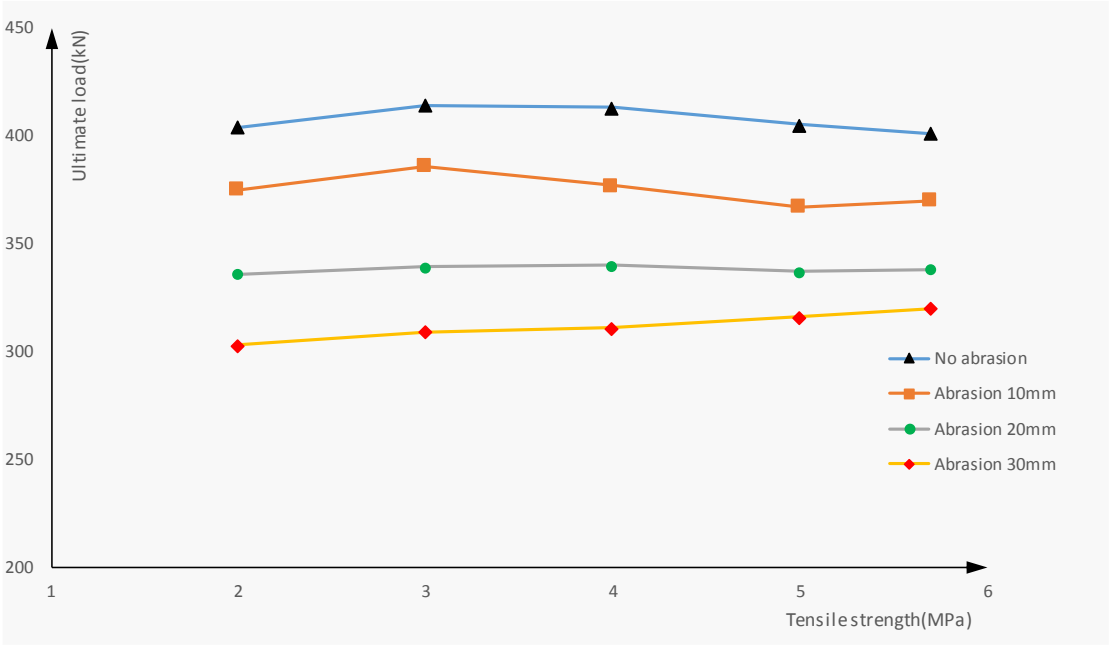

Fig. 17. Ultimate load of sleeper influenced by tensile strength of concrete

(3) Prestress loss rate

Since creep and shrinkage of concrete exist, the prestress losses along the whole life of concrete sleepers. In this study, the prestress loss rate is considered from 10% to 30%. The loading capacity of sleepers with different depth RSA can then be calculated and the results are given in Table 9. With the change in prestress loss rate, the cracking loads and ultimate loads for the sleepers with different RSA depth are shown in Fig. 18 and Fig. 19.

From Table 9, Fig. 18 and Fig. 19, it can be found that the cracking load of a sleeper with different depth RSA will decrease when the prestress loss increases. However, the ultimate load almost does not change with the prestress loss.

Table 9. Loading capacity of sleeper based on different prestress loss rate

Prestress loss rate	**Cracking load for different RSA depth (kN)**				**Ultimate for different RSA depth (kN)**			
(MPa)	**0**	**10mm**	**20mm**	**30mm**	**0**	**10mm**	**20mm**	**30mm**
10%	174	151	127	105	401	369	335	325
15%	166	145	124	103	406	362	333	323
20%	160	139	119	99.4	401	357	331	319

25%	154	134	114	97	401	358	332	320
30%	147	130	109	95	392	360	337	321

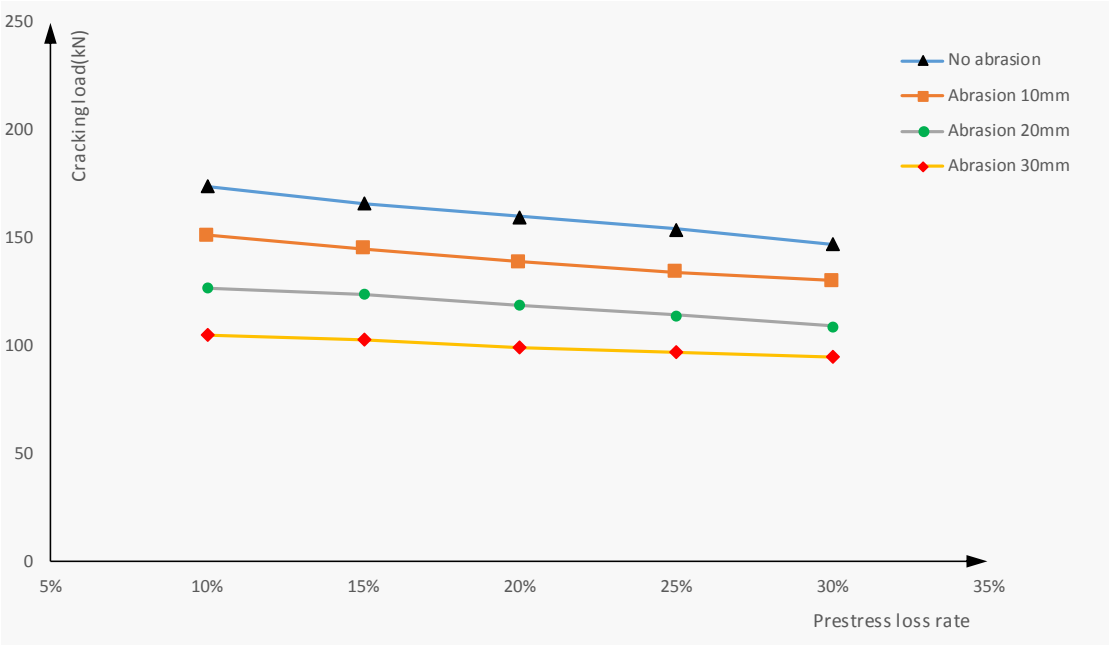

Fig. 18. Cracking load of sleeper influenced by prestressing loss rate

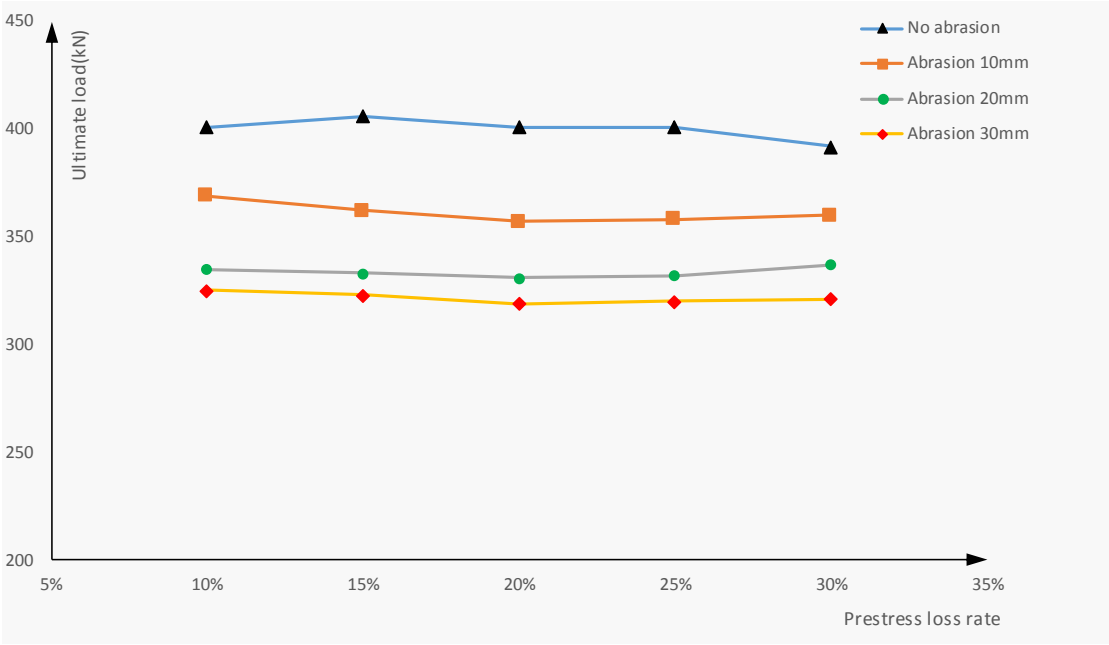

Fig. 19. Ultimate load of sleeper influenced by prestressing loss rate

6. Conclusions

This paper presents original, rigorous numerical and experimental investigations into the structural capacity of railway prestressed concrete sleepers with rail seat abrasion (RSA). RSA is one of the most common damages of a prestressed concrete sleeper in ballasted railway tracks, especially in freight operations. RSA is commonly related to axle load, traffic volume, curvature and grade of the rail line, the presence of abrasive fines (e.g. locomotive sand or metal shavings), the behaviour of the fastening system, and climate, etc. RSA results in many problems of railway tracks including the deteriorated quality of the track geometry and the reduced loading carry capacity of aging, worn concrete sleepers.

This study presents a nonlinear finite element model for determining the structural capacity of a prestressed concrete sleeper with RSA. This study is the world first to address the importance challenge towards truly realistic condition-based predictive track maintenance. The finite element model's crack and ultimate loads have been established and validated using comprehensive experimental results. The comparison results show that the simulations are in excellent agreement with the theoretical analyses (i.e. cross sectional analysis method) and experiment results. By using the validated finite element model, the influences of severity of RSA can be investigated. In addition, the effects of compression strength and tensile strength of concrete and the prestressing losses are highlighted. The outcomes of this study lead to better insight into the influences of RSA on railway concrete sleepers. The insight will significantly improve track maintenance and inspection criteria.

Acknowledgements

The first author wishes to thank the China Academy of Railway Sciences (CARS) for financial sponsorship of the collaborative project at the University of Birmingham (UoB) and is supported by Chinese Railway for Railway Technology Research Innovations Scheme, Project No. Z2016-028, 2015G004-A and 2016G003-C. The authors are grateful to the European Commission for H2020-MSCA-RISE, Project No. 691135 "RISEN: Rail Infrastructure Systems Engineering Network" (www.risen2rail.eu) [31].

References

[1] S. Kaewunruen, A.M. Remennikov. Impact capacity of railway prestressed concrete sleepers. Engineering Failure Analysis. 16 (2009) 1520-32.
[2] R. You, D. Li, C. Ngamkhanong, R. Janeliukstis, S. Kaewunruen. Fatigue Life Assessment Method for Prestressed concrete sleepers. Frontiers in Built Environment. 3 (2017) 1-13.
[3] C. Ngamkhanong, D. Li, S. Kaewunruen, Impact capacity reduction in railway prestressed concrete sleepers with vertical holes, IOP Conference Series: Materials Science and Engineering, IOP Publishing Ltd Prague, Czech Republic, 2017.
[4] S. Kaewunruen. Experimental and numerical studies for evaluating dynamic behaviour of prestressed concrete sleepers subject to severe impact loading. PhD Thesis, Wollongong, Australia: University of Wollongong; 2007.
[5] S. Kaewunruen, E.K. Gamage, A.M. Remennikov. Structural Behaviours of Railway Prestressed Concrete Sleepers (Crossties) With Hole and Web Openings. Procedia Engineering. 161 (2016) 1247-53.
[6] W. Ferdous, A. Manalo. Failures of mainline railway sleepers and suggested remedies – Review of current practice. Engineering Failure Analysis. 44 (2014) 17-35.
[7] C. Stuart. International Concrete Crosstie and Fastening System Survey. Research Results. (2013).
[8] M. Murray, Z. Cai. Literature review on the design of railway prestressed concrete sleeper. RSTA Research Report. (1998).
[9] J.C. Zeman. Hydraulic mechanisms of concrete-tie rail seat deterioration. Illinois, America: University of Illinois at Urbana-Champaign; 2010.

[10] C. Ngamkhanong, D. Li, S. Kaewunruen, Impact Capacity Reduction in Railway Prestressed Concrete Sleepers with Surface Abrasions, IOP Conference Series: Materials Science and Engineering, IOP Publishing, 2017, p. 032048.
[11] T. Bakharev, L. Struble. Microstructural features of railseat deterioration in concrete ties. Journal of materials in civil engineering. 9 (1997) 146-53.
[12] J.C. Zeman, J.R. Edwards, D.A. Lange, C.P. Barkan, Investigation of potential concrete tie rail seat deterioration mechanisms: cavitation erosion and hydraulic pressure cracking, Proceedings of the Transportation Research Board 89th Annual Meeting, Transportation Research Board, Washington, DC, 2010.
[13] S. Kaewunruen, A.M. Remennikov, Effect of a large asymmetrical wheel burden on flexural response and failure of railway concrete sleepers in track systems, Engineering Failure Analysis, 15, (2008): 1065-1075.
[14] K.J. Bakke, Abrasion resistance, Significance of Tests and Properties of Concrete and Concrete-Making Materials, ASTM International, West Conshohocken, PA, 2006, pp. pp.184–93.
[15] R.G. Kernes, A.A. Shurpali, J.R. Edwards, M.S. Dersch, D.A. Lange, C.P. Barkan. Investigation of the mechanics of rail seat deterioration and methods to improve the abrasion resistance of concrete sleeper rail seats. Proceedings of the Institution of Mechanical Engineers, Part F: Journal of Rail and Rapid Transit. 228 (2014) 581-9.
[16] S. Kaewunruen, C. Ngamkhanong, R. Janeliukstis, R. You, Influence of surface abrasions on dynamic behaviours of railway concrete sleepers, 24th International Congress on Sound and Vibrasiopn, International Congress on Sound and Vibrasiopn, London, United Kingdom, 2017, pp. 1-8.
[17] AS1085.14, Railway track material Part 14: Prestressed concrete sleepers, Standards Australia, Australia, 2003.
[18] A. Parvez. Fatigue behaviour of steel-fibre-reinforced concrete beams and prestressed sleepers Ph.D. Australia: The University of New South Wales; 2015.
[19] A. Parvez, S.J. Foster. Fatigue of steel-fibre-reinforced concrete prestressed railway sleepers. Eng Struct. 141 (2017) 241-50.
[20] T. Koh, M. Shin, Y. Bae, S. Hwang. Structural performances of an eco-friendly prestressed concrete sleeper. Construction and Building Materials. 102 (2016) 445-54.
[21] A.M. Keynia. Structural Analysis of Reinforced Concrete. Isfahan University of Technology Press, Iran, 1998.
[22] B.J. Winkelbauer, R.W. Bielenberg, J.D. Reid, M. Director, S.K. Rosenbaugh, Phase I Evaluation of Selected Concrete Material in LS-DYNA, NDOR Sponsoring Agency Contract, Lincoln, Nebraska, 2016, pp. 110-40.
[23] L. Schwer, The Winfrith concrete model: Beauty or beast? Insights into the Winfrith concrete model, 8th European LS-DYNA Users Conference, Livermore Software Technology Corp, Strasbourg, Frence, 2011, pp. 23-4.
[24] S. Minoura, T. Watanabe, M. Sogabe, K. Goto. Analytical Study on Loading Capacity of Prestressed Concrete Sleeper. Procedia Engineering. 199 (2017) 2482-7.
[25] N.S. Ottosen. A failure criterion for concrete. American Society of Civil Engineers. Engineering Mechanics Division. Journal. 103 (1977) 527-35.

[26] L.S.T. Corporation, LS-DYNA Keyword User's Manual, Version R 7.0, Livermore Technology Software Corporation (LSTC), Livermore,California, USA, 2013.
[27] Ngamkhanong C., Li D., Remennikov, A.M., Kaewunruen, S. Dynamic capacity reduction of railway prestressed concrete sleepers due to surface abrasions considering the effects of strain rate and prestressing losses, International Journal of Structural Stability and Dynamics. 2018; in press. https://doi.org/10.1142/S0219455419400017
[28] A. M. Remennikov, S. Kaewunruen, A review of loading conditions for railway track structures due to train and track vertical interaction, Structural Control and Health Monitoring, 15(2): 207-234, 2008.
[29] E.K. Gamage, S. Kaewunruen, A. Remennikov, and T. Ishida, Toughness of railroad concrete crossties with holes and web openings, Infrastructures 2, 3, 2017.
[30] E.K. Gamage, S. Kaewunruen, A. Remennikov, and T. Ishida, Reply to Giannakos, K. Comment on: Toughness of Railroad Concrete Crossties with Holes and Web Openings, Infrastructures 2, 3, 2017.
[31] Kaewunruen S, Sussman JM, Matsumoto A. Grand challenges in transportation and transit systems. Front Built Environ 2016; 2(4).